Available online at www.sciencedirect.com
SCIENCE DIRECT®
ELSEVIER
Nuclear Instruments and Methods in Physics Research A 541 (2005) 350–356
NUCLEAR INSTRUMENTS & METHODS IN PHYSICS RESEARCH Section A
www.elsevier.com/locate/nima

Development of the X-ray CCD camera for the MAXI mission

Haruyoshi Katayama[a,*], Hiroshi Tomida[a], Masaru Matsuoka[a], Hiroshi Tsunemi[b], Emi Miyata[b], Daisuke Kamiyama[b], Norbert Nemes[b]

[a]*Japan Aerospace Exploration Agency, Tsukuba Space Center, 2-1-1 Sengen, Tsukuba, Ibaraki 305-8505, Japan*
[b]*Department of Earth & Space Science, Graduate School of Science, Osaka University, 1-1 Machikaneyama, Toyonaka, Osaka 560-0043, Japan*

Available online 2 March 2005

Abstract

Monitor of All-sky X-ray Image (MAXI) is an astrophysical payload for the Japanese Experiment Module (Kibo) on the International Space Station (ISS). MAXI is designed for full-sky monitoring in the 0.5–30 keV X-ray band.

The Solid-state Slit Camera (SSC) is the X-ray CCD Camera for the MAXI mission. We have developed an engineering model (EM) of the SSC. Combined with the EM electronics, we achieved low readout noise ($\sim 5e^-$ rms) and good energy resolution (150 eV at 5.9 keV).

We also examine the energy scale and the energy resolution as a function of energy using our calibration system. From these results, we conclude that the performance of the SSC-EM almost fulfills our requirements and that the final performance goals will be obtained in the flight model.

PACS: 07.85.−m; 95.55.−n; 95.55.Aq; 95.55.Ka

Keywords: X-ray Astronomy; X-ray CCD; International Space Station; MAXI

1. Introduction

The Monitor of All-sky X-ray Image (MAXI) [1–4] payload has been selected as one of the first-generation payloads that will be attached to the Japanese Experiment Module (Kibo)-Exposed Facility (JEM-EF), a component of the International Space Station (ISS). MAXI is currently planned for launch by an H-IIA Transfer Vehicle (HTV) in 2008 and is expected to have a mission life of at least two years in orbit. This payload is designed for full sky monitoring in the 0.5–30 keV X-ray band.

MAXI consists of two X-ray detector systems: the gas slit camera (GSC) [5,4] and the Solid-state Slit Camera (SSC) [6]. These are combinations of a narrow slit, a collimator, and a one-dimensional position-sensitive detector. The energy ranges

*Corresponding author.
E-mail address: Katayama.Haruyoshi@jaxa.jp (D. Kamiyama).

0168-9002/$ - see front matter © 2005 Elsevier B.V. All rights reserved.
doi:10.1016/j.nima.2005.01.075

of the GSC and the SSC are 2–30 keV and 0.5–10 keV, respectively. In this paper, we describe the performance of the engineering model (EM) of the MAXI/SSC.

2. SSC overview

The SSC is developed by JAXA, Osaka University, and Mesei Electric Co., Ltd. The SSC uses an X-ray CCD to achieve a high quantum efficiency and a good energy resolution for soft X-rays. The total imaging area of the SSC is 200 cm^2 and it consists of two camera units, viewing both the horizontal (SSC-H) and zenith (SSC-Z) directions. Fig. 1 shows a schematic view of the two camera units of the SSC. The field of views (FOVs) of the two cameras are set almost perpendicular to each other to achieve complete sky coverage in spite of breaks in the observations when the ISS passes through radiation belts such as the South Atlantic Anomaly. The FOV of SSC-H is tilted upward by 20° to avoid earth occultation and light reflection from the earth in daytime. The FOV of each camera is restricted to $1.5 \times 90^\circ$ with a combination of a slat collimator and a slit. Fig. 2 (left) shows the slat collimator of the SSC viewed from the bottom side (CCD side). The collimator slat is made up of phosphorus bronze (Cu: 93.9%, Sn: 6.0%, and P: 0.1%), and its surface is etched and coated black for light shielding.

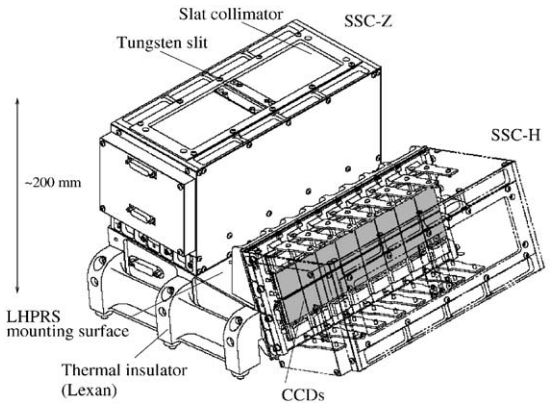

Fig. 1. Schematic view of two camera units of the SSC, where the colored region represents 16 CCD chips.

Each of the SSC cameras consists of 16 CCD chips. Fig. 2 (right) shows the SSC Engineering Model (EM) without its collimator. The CCD chip (FFTCCD–4673) fabricated by Hamamatsu Photonics K.K. has 1024×1024 pixels with a pixel size of 24 μm and covers 25 mm square. The thickness of the depletion layer is 70 μm. On the surface of the CCD, an aluminum layer ~ 2000 Å thick has been deposited for light shielding. This permits omission of an additional light shield, like an optical blocking filter, and its associated launch safety mechanism. The CCD is damaged by soft protons in orbit, resulting in a decrease of the charge transfer efficiency. The SSC CCD contains a charge injection register for the purpose of recovery from this radiation damage. The effect of the radiation damage in the two years of MAXI mission is examined in Ref. [7].

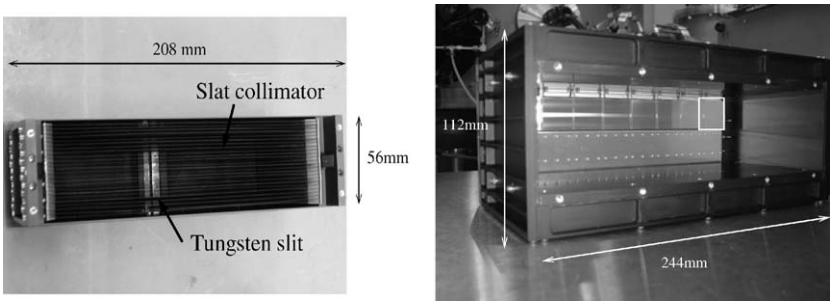

Fig. 2. Left: Slat collimator of the SSC viewed from the bottom side (CCD side). Right: A view of SSC-EM, with the collimator not installed. On the bottom plate are mounted 7 out of 16 CCDs. The remaining 9 CCDs were installed in Oct. 2004. A white square represents the size of 1 CCD chip.

Table 1
Basic properties of the MAXI/SSC

CCD chip (*FFTCCD-4673*)	
Pixel size	24 μm
Number of pixels	1024 × 1024
Depletion layer thickness	70 μm
Operation temperature	<-60 °C
Charge transfer rate	125 kHz/62.5 kHz[a]
Camera	
Energy range	0.5–10 keV
Energy resolution	$\leqslant$150 eV at 5.9 keV
Number of CCDs	16 × 2
Field of view	1.5 × 90° × 2
Effective imaging area	100 cm^2 × 2

[a]The nominal charge transfer rate is 125 kHz, but it can be reduced to 62.5 kHz if required.

To achieve the required energy resolution (150 eV FWHM at 5.9 keV), the CCDs are cooled below −60 °C using a combination of a radiator and a one-stage Peltier cooler. The Peltier cooler, attached directly to each CCD, provides a temperature difference of −40 °C between a hot side and a cold side for 1 W of power. The hot side of the Peltier cooler is cooled below −20 °C by the loop heat pipe radiation system (LHPRS) [8].

We summarize the basic properties of the MAXI/SSC in Table 1.

3. Calibration system of SSC

We evaluated the performance of the SSC-EM with a calibration system constructed at JAXA. This MAXI calibration system is described in Ref. [9]. The SSC calibration system, which uses fluorescent X-rays, is shown in Fig. 3. The compact X-ray generator (KEVEX) can be operated from 5 to 10 kV and at a maximum current of 1 mA. The X-ray generator is connected to a secondary target chamber. We employ Al, Cl, Ti, V, Fe, Ni, and Zn as secondary targets. These secondary X-rays are then incident on the SSC installed in a large chamber. The SSC is cooled down using a cryogenic cooler. Each of the two chambers is evacuated to less than $\sim 10^{-5}$ Torr by turbo molecular and rotary pumps. The SSC is cooled to −20 °C in the SSC chamber, while the SSC Electronics is operated at about ~20 °C, the nominal temperature in orbit.

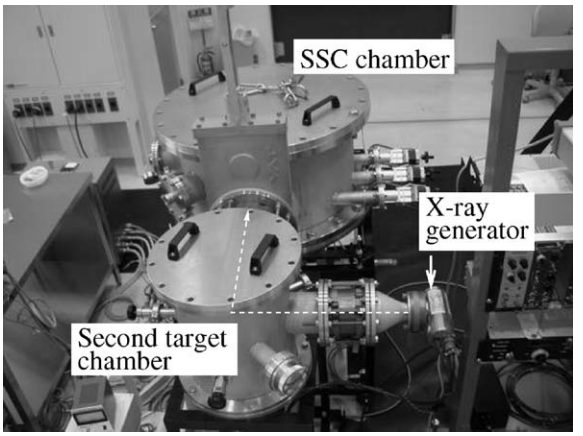

Fig. 3. Calibration system of the SSC. X-rays from the X-ray generator are incident on a secondary target. Fluorescent X-rays from this secondary target are emitted to the SSC, installed in a larger chamber as indicated.

4. Performance of the SSC engineering model

We used 7 CCD chips for the evaluation of the EM (Fig. 2 (right)). These are almost the same type as the flight CCD chips, though the thicknesses of depletion layer of these CCDs are thinner than those of the flight CCDs.

We first examined the basic performance of the SSC-EM using a ^{55}Fe source. Fig. 4 shows the spectrum of ^{55}Fe taken with the SSC-EM. The readout noise is determined from a region of oversampled pixels. The readout noise and energy resolution at 5.9 keV for the 7 CCDs are listed in Table 2. The readout noise is 5−6 e^- for all CCDs. These fulfill our requirement. The energy resolution of 3 CCDs (CCDID = 4,5,6) are worse than our requirement. This is mainly due to variation of the charge transfer efficiency of these CCDs. However, the flight CCD chips, which are not installed in the EM but planned to be installed in a flight model, show energy resolutions below 150 eV [10].

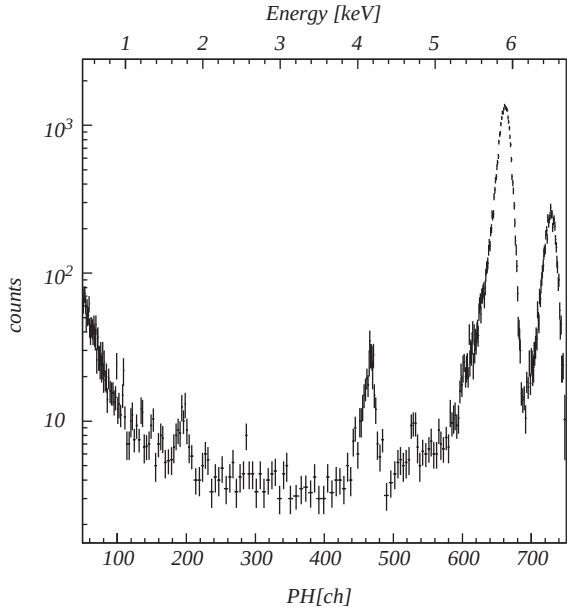

Fig. 4. Pulse-height spectrum for a ^{55}Fe source taken with the SSC-EM. Single pixel events (ASCA grade of 0) are selected for this distribution, as described in the text.

Table 2
Basic performance of the 7 CCDs of the SSC-EM. The operating temperature is −60 °C

CCDID	Readout noise (e^- rms)	FWHM (eV)[a]
0	5.4 ± 0.4	143 ± 4
1	5.7 ± 0.2	145 ± 3
2	5.7 ± 0.2	156 ± 3
3	5.1 ± 0.2	145 ± 5
4	5.3 ± 0.2	194 ± 5
5	5.2 ± 0.2	163 ± 3
6	5.7 ± 0.2	160 ± 3

[a]Full-width at half-maximum at 5.9 keV.

4.1. Energy response (spectrum)

Fig. 5 shows the spectra of fluorescent X-rays from Al, Cl, Ti, V, Fe, Ni, and Zn taken with the SSC-EM. These are spectra of single pixel events with a split event threshold of 4 times the readout noise. Except for the Al case, the Kα and Kβ peaks are clearly resolved. In addition to the main peak, we can see a low-energy tail, which increases towards lower energies. This low-energy tail is considered to originate from photons absorbed inside the gate insulator of the CCD, as discussed in an ACIS calibration report [11] (Chandra/ACIS) and Ref. [12] (ASTRO-E/XIS). The MAXI/SSC low-energy tail shows similar trends with these CCDs, though its level is slightly higher (about 2 times). One possible explanation is the difference in the CCD gate thicknesses. Since the level of the low-energy tail depends on the gate thickness, a thicker gate leads to a larger low-energy tail. A quantum efficiency measurement, which will be measured in a next calibration experiment, will reveal it. We should note that the low-energy tail is not due to scattering X-rays from the vacuum chamber because the level of the low-energy tail of these spectra is about the same as that of the ^{55}Fe spectrum (see Fig. 4).

We fitted these spectra with a double Gaussian added on a constant term to derive the energy scale and the energy resolution of the SSC-EM.

4.2. Energy scale

We show the energy scale of the SSC-EM in Fig. 6 (left). We fitted the energy scale with a linear function. The lower panel in Fig. 6 shows the residuals from the linear energy scale fit. Except for the Al line, the residuals are within 0.1%. Since our calibration goal is to determine the energy scale with 0.1% accuracy, this result almost fulfills our requirement.

4.3. Energy resolution

Fig. 6 (right) shows the energy resolution of the SSC-EM as a function of energy. We define the energy resolution as the full width at half maximum (FWHM) of the main peak, and fit it with the following formula:

$$\mathrm{FWHM\ (eV)} = w \times \sqrt{8\ \log 2} \times \sqrt{\frac{F \times E}{w} + \sigma_0^2} \quad (1)$$

where w (we fixed 3.65 eV/e^-) is the mean ionization energy per one electron–hole pair, F is the Fano factor, and σ_0 is a measure of the system noise including the readout noise.

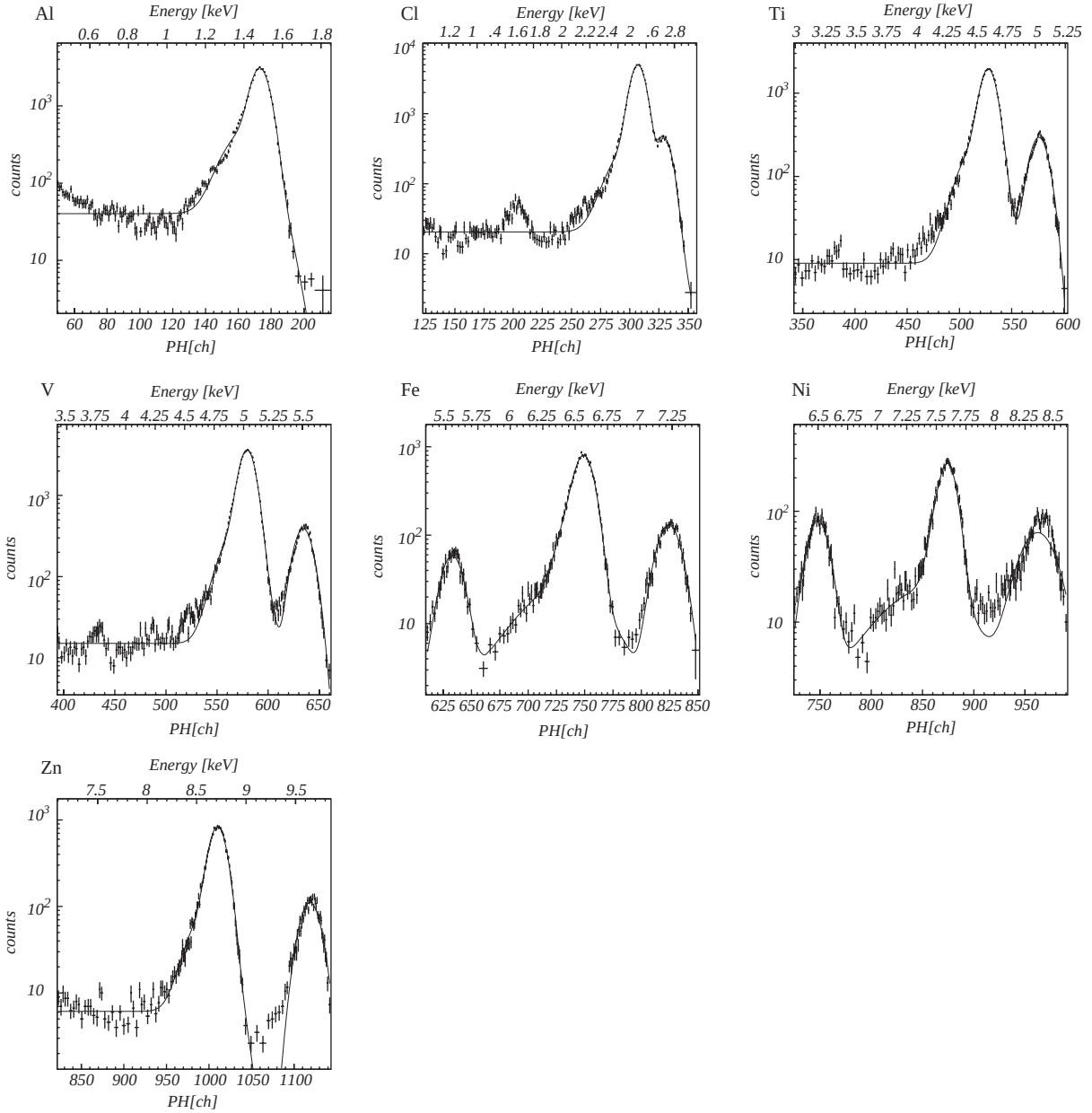

Fig. 5. Fluorescent X-rays spectra from Al, Cl, Ti, V, Fe, Ni, and Zn as measured by the SSC-EM. Except for the Al lines, the Kα and Kβ peaks are clearly resolved. A solid line represents the best fit to a double Gaussian added on a constant term. Also included in the Fe and Ni fits are Cr and Fe lines, respectively, which are contamination from the secondary targets. The Kβ peak of these lines is superposed on the tail of the Kα peak of the target lines.

One of the unique scientific goals of the SSC is X-ray emission-line mapping of our Galaxy. To archive this goal, the energy resolution in the soft X-ray band is important. From the best-fit parameters ($F = 0.167 \pm 0.003$ and $\sigma_0 = 7.85 \pm 0.19$), we estimate the energy resolution at

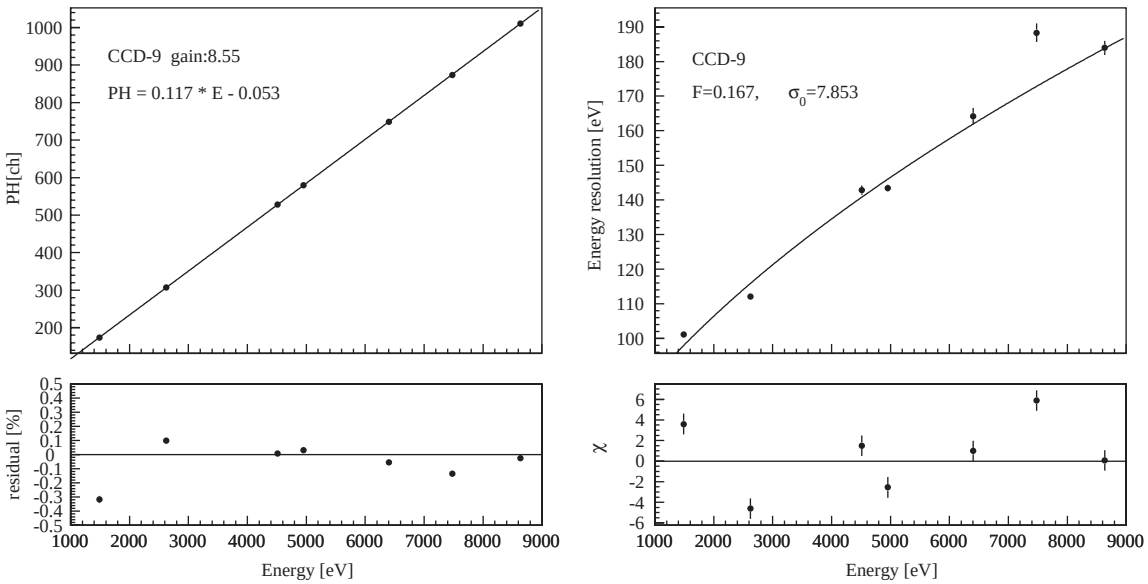

Fig. 6. Left: Energy scale of the SSC-EM. The data for Kα lines are plotted. The pulse-height is the center of the main peak fitted with a double Gaussian. The lower panel shows the residuals, which are within 0.1% except for the Al line. Right: Energy resolution of the SSC-EM, with fit goodness plotted in the lower panel.

the oxygen line energy (~ 0.53 keV) to be 80 eV at 0.5 keV, which is higher than the expected energy resolution of 60 eV for a readout noise of $5\,e^-$. This is represented by the large σ_0, which suggests that unknown noise sources are dominant, or there is an uncertainty in the energy response below the Al line. Although the O VII (~ 0.56 keV) and O VIII (~ 0.65 keV) lines can be resolved even with 80 eV energy resolution at 0.5 keV, in order to investigate this issue, we are now planning an experiment using a soft X-ray generator, which can provide X-ray irradiation below 2 keV.

5. Conclusion

We have developed an engineering model of the MAXI/SSC. Combined with the EM electronics, we achieved low readout noise ($\sim 5\,e^-$ rms) and good energy resolution (150 eV at 5.9 keV). We also examined the energy scale and the energy resolution as a function of energy using our calibration system. From these results, we conclude that the performance of the SSC-EM almost fulfills our requirements and that the final performance goals will be obtained in the flight model.

Acknowledgements

This work is partly supported by the Grant-in-Aid for Scientific Research by the Ministry of Education, Culture, Sports, Science and Technology of Japan (15684002).

References

[1] T. Mihara, et al., Adv. Space Res. 25 (2000) 897.
[2] S. Ueno, et al., ASP Conf. Ser. 251: New Century of X-ray Astronomy (2001) 598.
[3] M. Matsuoka, AAS/High Energy Astrophys. Div. 7 (2003).
[4] N. Isobe, et al., Proc. SPIE 5165 (2004) 354.
[5] T. Mihara, et al., Proc. SPIE 4497 (2002) 173.

[6] E. Miyata, C. Natsukari, D. Akutsu, M. Ohtani, H. Tsunemi, M. Matsuoka, N. Kawai, Proc. SPIE 4012 (2000) 186.
[7] E. Miyata, et al., Proc. SPIE 4851 (2003) 1080.
[8] M. Muto, H. Nagai, M. Murakami, S. Ueno, M. Matsuoka, Proceedings of the 32nd International Conference on Environment System (2002) 2505.
[9] K. Torii, et al., Proc. SPIE 3765 (1999) 636.
[10] E. Miyata, D. Kamiyama, H. Kouno, N. Nemesh, H. Tomida, H. Katayama, H. Tsunemi, M. Matsuoka, Proc. SPIE 5165 (2004) 366.
[11] M.W. Bautz, J.A. Nousek, G.P. Garmire, Tech. Rep., MIT 1999.
[12] K. Imanishi, H. Awaki, T.G. Tsuru, K. Hamaguchi, H. Murakami, M. Nishiuchi, K. Koyama, Proc. SPIE 4012 (2000) 137.